

Supplemental Information

Brief reports

The Mechanism of Anti-CD20-Mediated B-cell Depletion Revealed by Intravital Imaging

Fabricio Montalvao^{1,2}, Zacarias Garcia^{1,2}, Susanna Celli^{1,2}, Béatrice Breart^{1,2},
Jacques Deguine^{1,2}, Nico Van Rooijen³ and Philippe Bousso^{1,2,*}

Supplemental Methods

Partial hepatectomy and splenectomy

For partial hepatectomy, mice were anesthetized and a transverse abdominal incision was made. The superior lobes of the liver were laid on the diaphragm and the ligaments of the caudate lobe dissected. The caudate lobe was then pulled in front of the stomach and resected after in bloc ligature of its hilum (6/0 silk). The lateral left lobe was resected using the same technique. The abdomen was closed using 4/0 silk running sutures. The procedure removed approximately half of the initial liver mass. For splenectomy, the vessel of the splenic anterior extremity was tied (0/8 silk) and cut. The splenic ligaments were cut and the spleen gently pulled outside the abdomen. The vessels of the spleen posterior extremity were tied (0/8 silk) and cut.

Antibodies

Staining were performed using the following conjugated mAb: B220 (RA3-6B2), CD16/32 (93), CD19 (1D3), CD11b (M1/70), CD45 (30F11), Gr-1 (RB6-8C5), F4/80 (BM8), IgM (II/41) (eBioscience), CD64 (X54-5/7.1), Ly6G (1A8) (Biologend). Polyclonal MerTK Ab was purchased from R&D systems.

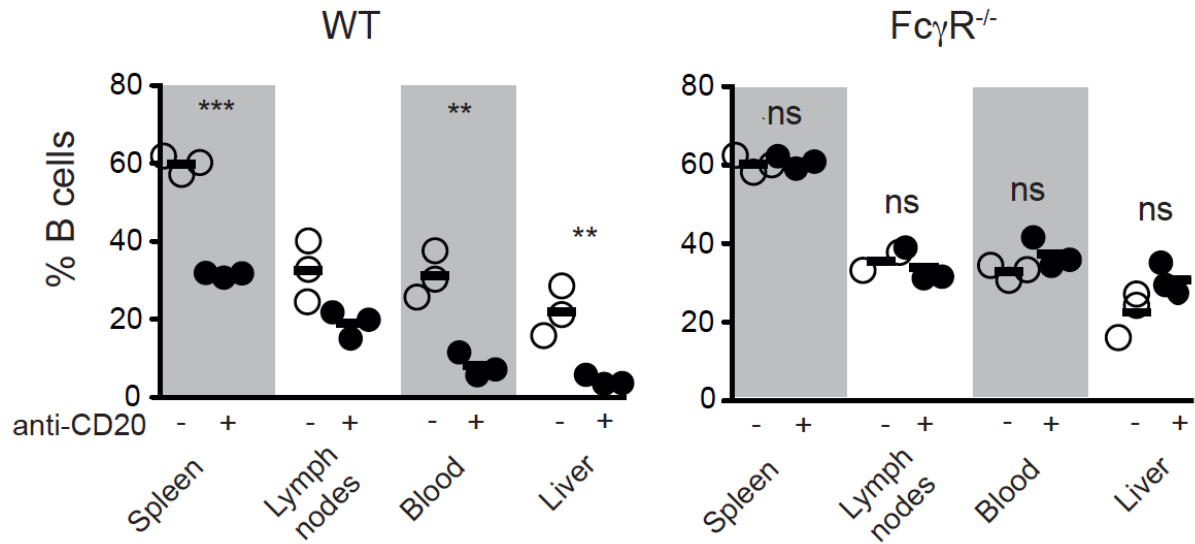
Generation of a fluorescent tumor B cell line

Lymph nodes cells from a lymphoma-bearing E μ -myc mice were retrovirally transduced with a CFP-DEVD-YFP construct. Transduced cells were selected on a FACSAria II (BD Biosciences) on the basis of YFP expression and further propagated as a stable cell line. Recipient mice were injected i.v. with 1.5×10^5 tumor cells and subjected to intravital imaging of the liver 3 weeks later.

Immunofluorescence

Perfused livers were cut, fixed overnight in paraformaldehyde and progressively dehydrated in sucrose. Tissues were snap frozen in OCT compound (Tissue-Tek; Sakura). 8- μ m-thick tissue sections were stained for F4/80 and B220, and imaged using a confocal microscope (Olympus BX61WI) with a 40X objective.

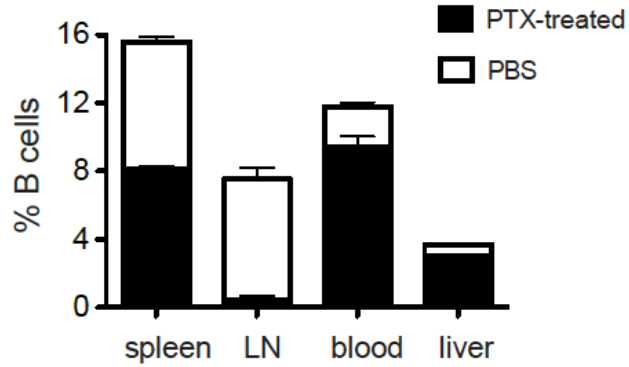
Supplementary Figures



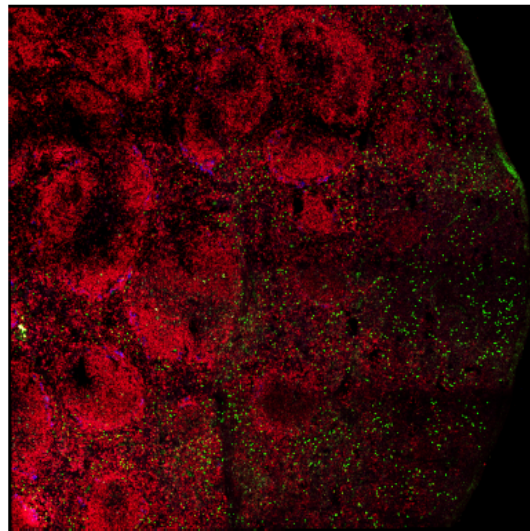
Supplemental Figure 1: Systemic B cell depletion following anti-CD20 treatment.

WT or FcγR^{-/-} mice were injected intravenously with a single dose of anti-CD20 Ab. After 16 hr, the percentage of B cells in the indicated organs was analyzed by flow cytometry. Each symbol corresponds to an individual mouse. Results are representative of two independent experiments.

A



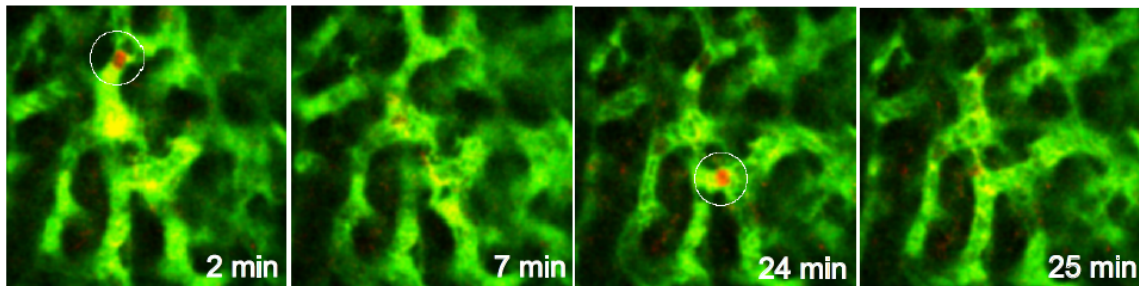
B



B220 PTX-treated splenocytes

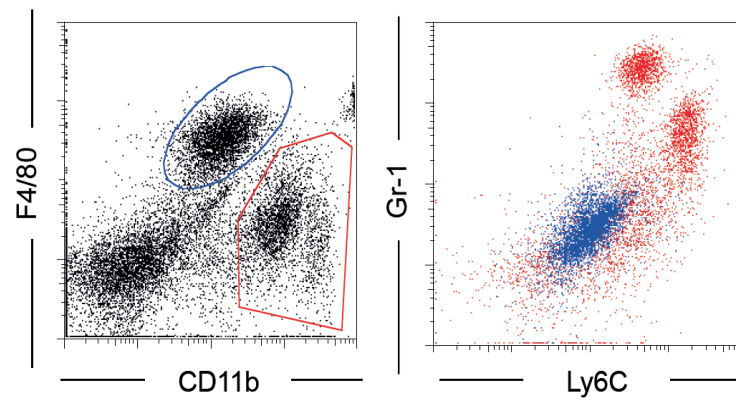
Supplemental Figure 2: PTX-treated B cells accumulate in the circulation

A) GFP⁺ PTX-treated and GFP⁻ untreated splenocytes were injected at a 1:1 ratio into *Rag2*^{-/-} recipients. Percentage of B cells was evaluated in the indicated organs 16 h after transfer. Results are representative of two independent experiments. B) PTX-treated splenocytes reach the red but not the white pulp of the spleen. PTX-treated splenocytes isolated from a GFP transgenic mouse were adoptively transferred. Immunofluorescence of frozen spleen sections at 24 hr after transfer shows that GFP⁺ cells are restricted to the red pulp.



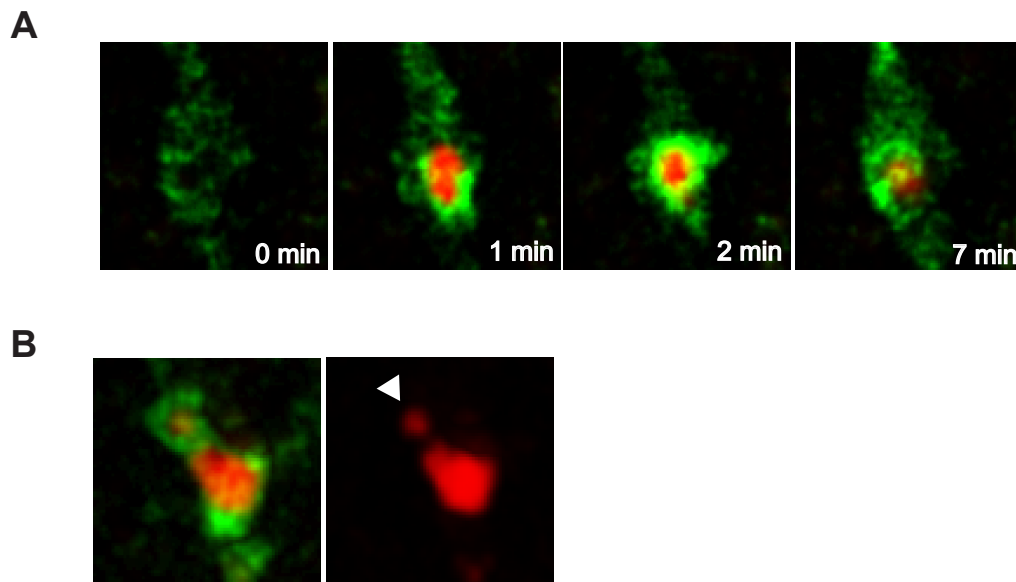
Supplemental Figure 3: B cell circulation in the liver sinusoids

Mice with RFP-expressing B cells were subjected to intravital imaging of the liver after i.v. injection of 70 KDa Dextran-FITC to label blood vessels.



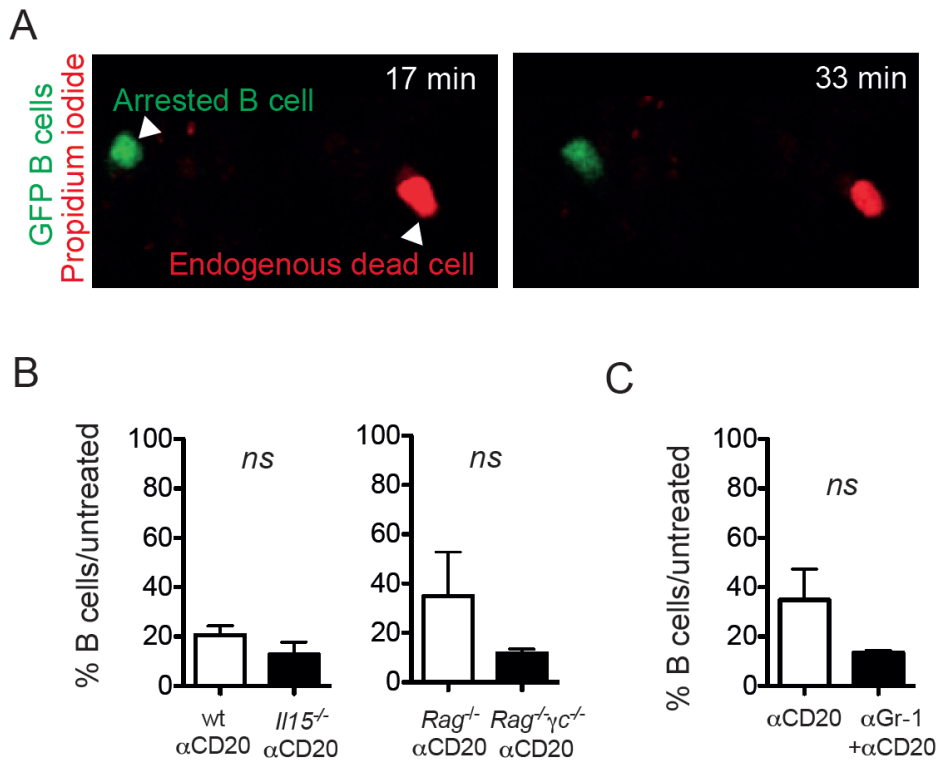
Supplemental Figure 4: Phenotypic analysis of liver cells

Phenotypic analysis of liver cells showing that CD11b^{high}F4/80^{low} cells (red gate) include both Ly6C⁺ monocytes and neutrophils (Gr-1^{high}). Kupffer cells (blue gate) correspond to F4/80^{high}CD11b^{low}Gr-1^{low}Ly6C^{low/-}.



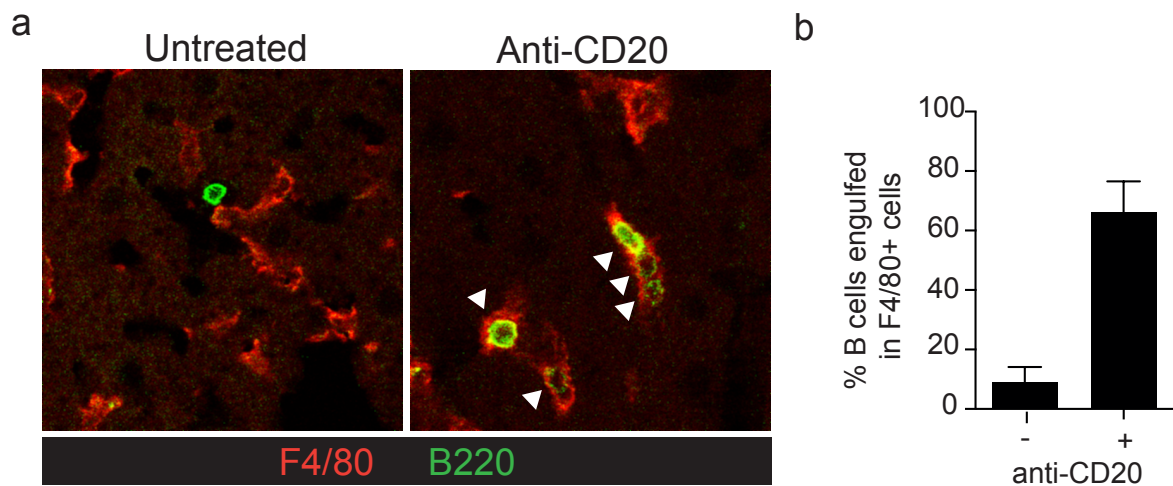
Supplemental Figure 5: Kupffer cells mediate the arrest and engulfment B cells during anti-CD20 therapy

Rag2^{-/-} MAFIA mice were adoptively transferred with Cell tracker Orange-labeled B cells and subjected to intravital imaging of the liver. **(A)** Zoom-in view showing the arrest of a B cell (red) on a Kupffer cell (green) following anti-CD20 injection and its subsequent engulfment. **(B)** Visualization of B cell debris following engulfment by Kupffer cells.



Supplemental Figure 6: B cells are not killed prior to phagocytosis during anti-CD20 treatment

A) GFP expressing B cells were transferred to *Rag^{-/-}* mice. Mice were injected intravenously with anti-CD20 Ab and with propidium iodide (PI) to label dead cells and were subjected to intravital imaging of the liver. Representative time-lapse images showing that PI labels some endogenous dead cells (GFP⁻) in the liver but does not label B cells that arrest in response to anti-CD20 treatment. B) Efficient anti-CD20-mediated B cell depletion in the absence of NK cells. Wild-type, NK cell deficient *Il15^{-/-}* or *Rag^{-/-}γc^{-/-}* mice were injected intravenously with a single dose of anti-CD20 Ab. After 16 hr, the percentage of B cells in the blood was measured by flow cytometry and compared to that of recipients that did not receive anti-CD20. C) Efficient anti-CD20-mediated B cell depletion in the absence of granulocytes. Mice were treated or not with anti-Gr-1 Ab to deplete granulocytes. After 24h, mice were injected with a single dose of anti-CD20 Ab. After 16 hr, the percentage of B cells in the blood was measured by flow cytometry.



Supplemental Figure 7: Engulfment of liver B cells by F4/80⁺ cells upon anti-CD20 treatment

Mice were treated with anti-CD20 or left untreated. After 1 hr, livers were harvested and immunofluorescence was performed on frozen liver sections. a) Representative images corresponding to F4/80 and B220 staining in liver sections of untreated and treated mice. Arrows indicate B cells engulfed by F4/80⁺ cells. b) Quantification of B cell engulfment in response to anti-CD20. The percentage of liver B cells found inside F4/80⁺ cells is displayed. Representative of two independent experiments.

Legends for supplemental movies

Movie 1: B cells circulation in the liver sinusoids

Mice with RFP-expressing B cells (*Cd19^{cre/cre}* x *Rosa26^{RFP/+}*) were subjected to intravital imaging of the liver following i.v. injection of fluorescent dextran to label the vasculature.

Movie 2: Anti-CD20 injection induces the abrupt arrest of B cells in the liver

Mice with RFP-expressing B cells (*Cd19^{cre/cre}* x *Rosa26^{RFP/+}*) were subjected to intravital imaging of the liver. B cells behavior was recorded before or immediately after anti-CD20 injection. B cells are shown in red.

Movie 3: Sessile GFP⁺ cells in the liver of MAFIA mice correspond to Kupffer cells

MAFIA mice were injected i.v. with PE-conjugated anti-F4/80 and subjected to intravital imaging of the liver 10 min later. Note that sessile GFP⁺ cells display the typical KC morphology and express F4/80. In contrast, motile GFP⁺ cells are not stained with F4/80. GFP⁺ cells are shown in green, F4/80 staining in red.

Movie 4: B cells made only transient interactions with Kupffer cells in the liver in the absence of anti-CD20

Rag2^{-/-} MAFIA mice were adoptively transferred with Cell tracker Orange-labeled B cells and subjected to intravital imaging of the liver. GFP⁺ cells are shown in green, B cells in red.

Movie 5: Kupffer cells mediate the arrest and engulfment of liver B cells following anti-CD20 injection

Rag2^{-/-} MAFIA mice were adoptively transferred with Cell tracker Orange-labeled B cells and subjected to intravital imaging of the liver immediately after anti-CD20 injection. Note that B cells arrest on KCs and are rapidly engulfed. GFP⁺ cells are shown in green, B cells in red.

Movie 6: Kupffer cells mediate the depletion of tumor cells in the liver following anti-CD20 treatment

MAFIA mice were injected with a fluorescent B cell tumor line and 3 weeks later subjected to intravital imaging of the liver before (left) or immediately after (right) injection of anti-CD20. GFP⁺ cells are shown in green, tumor cells in red.